JOURNAL OF MOLECULAR RECOGNITION
J. Mol. Recognit. 1999;**12**:3–18

Review

Isothermal titration calorimetry and differential scanning calorimetry as complementary tools to investigate the energetics of biomolecular recognition

Ilian Jelesarov* and Hans Rudolf Bosshard

Department of Biochemistry, University of Zurich, CH-8057 Zurich, Switzerland

The principles of isothermal titration calorimetry (ITC) and differential scanning calorimetry (DSC) are reviewed together with the basic thermodynamic formalism on which the two techniques are based. Although ITC is particularly suitable to follow the energetics of an association reaction between biomolecules, the combination of ITC and DSC provides a more comprehensive description of the thermodynamics of an associating system. The reason is that the parameters ΔG, ΔH, ΔS, and ΔC_p obtained from ITC are global properties of the system under study. They may be composed to varying degrees of contributions from the binding reaction proper, from conformational changes of the component molecules during association, and from changes in molecule/solvent interactions and in the state of protonation.

Keywords: **isothermal titration calorimetry; differential scanning calorimetry**

Received 1 June 1998; accepted 15 June 1998

Introduction

Specific binding is fundamental to the molecular organization of living matter. Virtually all biological phenomena depend in one way or another on molecular recognition, which either is *inter*molecular as in ligand binding to a macromolecule and in the formation of macromolecular complexes, or *intra*molecular as in protein folding. Here we deal with intermolecular recognition, that is, with binding reactions. The specificity and precision of binding reactions has fascinated biologists and chemists from the very beginning of modern biochemistry, and one of the most rapidly advancing fields today is the study of molecular recognition between macromolecules. The quantitative description of the forces that govern the formation of biomolecular complexes is part of this endeavor. It has great practical significance to the knowledge-based development of new drugs, vaccines and other medicinal compounds.

The number of high resolution crystal structures of biomolecular complexes is growing fast and there is a large data base describing the complementarity of interacting surfaces and the precise orientation of interacting groups. From the many detailed, yet static, pictures of biomolecular complexes we have learned *how* molecules interact, but we less well know *why* they do so. This means we have to find ways to rationalize structure in terms of energetics, a task that still is enormously difficult inspite of some very promising theoretical developments and of the steady accumulation of experimental results. Theoretical concepts have developed in the tradition of physical-organic chemistry. It is difficult to adapt these concepts in a straightforward way to complex biomacromolecules. Proteins and nucleic acids are so large that in solution they may be regarded as individual macroscopic systems surrounded by solvent (Privalov and Potekhin, 1986). They behave cooperatively and often undergo structural rearrangements during binding reactions. The changes range from the subtle adjustments of dihedral angles to the prominent rearrangement and even refolding of entire molecular domains (Padlan, 1996). For example, in a DNA binding protein the domain that binds to the DNA target site can be unstructured in the free protein and becomes folded only when it is bound to DNA (Patikoglou and Burley, 1997). The energetic consequence of such binding-induced refolding is far from being understood, but the energetic cost is thought to be large. From this perspective, binding specificity has to be redefined. It is no longer a simple function of spatial complementarity and of accumulation of favorable interactions between molecules that can be treated as rigid bodies. Binding between large and flexible biomolecules has a complicated energy profile involving different energetic expenditures in going from the free components to the final complex. The free energy of complex formation turns out to be a very small number resulting from a delicate balance between large favorable and large unfavorable contributions. Moreover, binding takes place only if the *total* free

* Correspondence to: I. Jelesarov, Department of Biochemistry, University of Zurich, Winterthurerstrasse 190, CH-8057 Zurich, Switzerland.

Abbreviations used: DSC, differential scanning calorimetry; ITC, isothermal titration calorimetry.

 CCC 0952–3499/99/010003–16 $17.50

energy change decreases, regardless of the actual amount of favorable free energy change accumulated by direct molecular contact between the associating biomolecules. This is to say, solvent effects are as important to the energy balance as are direct noncovalent interactions (Collins, 1997; Jelesarov *et al.*, 1998).

Basic Thermodynamic Relationship Describing Binding Phenomena

The Gibbs free energy change, ΔG, of an association reaction is temperature dependent and is described by

$$\Delta G(T) = \Delta H(T_R) + \int_{T_R}^{T} \Delta C_p dT - T\Delta S(T_R) - T\int_{T_R}^{T} \Delta C_p d\ln T \quad (1)$$

ΔH and ΔS are the change in enthalpy and entropy, respectively, ΔC_p is the heat capacity change, and T_R is an appropriate reference temperature. If ΔC_p is temperature-independent in the temperature interval of interest, Eq. (1) simplifies to

$$\Delta G(T) = \Delta H(T_R) - T\Delta S(T_R) + \Delta C_p[T - T_R - T\ln(T/T_R)] \quad (2)$$

Equations (1) and (2) show that the free energy of association has an enthalpy and an entropy component. The changes of enthalpy and entropy depend on temperature according to

$$\Delta C_p = \frac{d(\Delta H)}{dT} = T\frac{d(\Delta S)}{dT} \quad (3)$$

To characterize the thermodynamics of a binding reaction means to determine ΔG, ΔH and ΔS at a given reference temperature and to obtain ΔC_p to predict the change of the above three parameters with temperature.

Non-calorimetric determination of binding energetics

ΔG is accessible through many types of binding experiments because ΔG is related to the association constant K_A by $\Delta G = -RT \ln K_A$ where R is the gas constant (8.314 J $K^{-1}mol^{-1}$) and T is the absolute temperature in degrees Kelvin. In the simplest case a molecule L reacts with another molecule M to the complex ML.[1] The association constant is $K_A = [ML]/[M][L]$ where the brackets indicate concentration expressed in units of mol l^{-1} and K_A has units of l mol^{-1}. To take the logarithm, K_A must be a dimensionless ratio. This is achieved by normalizing the molar concentrations to the standard state concentration of 1 mol l^{-1}. Alternatively, K_A can be expressed as (mol fraction)$^{-1}$, where 1 mol l^{-1} equals 1.8×10^{-2} mol fraction (corresponding to 1/55.56 mol H_2O per 1). The choice of the standard state is a matter of convention yet is important when comparing values of ΔG and ΔS.

There are many ways to measure K_A. Let us begin with the simple equilibrium between L, M and ML:

$$L + M \underset{\longleftarrow}{\overset{K_A}{\longrightarrow}} ML$$

Techniques like equilibrium dialysis, ultracentrifugation, or radio-ligand binding assay directly yield values for [ML], [M], or [L] to calculate K_A. More indirect and mostly spectroscopic methods yield an observable p the change of which is proportional to the degree of saturation, Y, according to:

$$Y = \frac{\Delta p_i}{\Delta p_{max}} = \frac{[ML]}{[M] + [ML]} = \frac{K_A[L]}{1 + K_A[L]} \quad (4)$$

Δp_i is a signal change (e.g. a change of fluorescence accompanying the formation of the complex, ML), and Δp_{max} is the maximum signal change at full saturation ($Y = 1$). From Y measured at different temperatures, $K_A(T)$ and $\Delta G(T)$ are obtained. $\Delta H(T)$ and $\Delta S(T)$ can be derived using the integrated form of the van't Hoff equation:

$$\int_{T_1}^{T_2} d\ln K_A = \int_{T_1}^{T_2} \frac{\Delta H}{RT^2} dT \quad (5a)$$

and

$$\int_{T_1}^{T_2} \Delta G = -\int_{T_1}^{T_2} \Delta S dT \quad (5b)$$

Further, taking the second derivative of $\Delta G(T)$ with respect to temperature, one obtains ΔC_p. The non-calorimetric approach to the thermodynamics of an association reaction, commonly called a van't Hoff analysis, has severe drawbacks. First, for technical reasons, experiments can be performed only in a limited temperature range, and experimental errors propagate into large errors of ΔH, ΔS, and of ΔC_p in particular. Second, K_A very often appears temperature-independent in the experimentally accessible T-range because of enthalpy/entropy compensation between large and strongly temperature-dependent ΔH and ΔS. Therefore, the van't Hoff analysis of a binding reaction is often flawed.

Isothermal Titration Calorimetry

ITC and DSC are the only methods for the direct determination of ΔH. The principle of ITC is now reviewed first. It is the most direct method to measure the heat change on formation of a complex at constant temperature. Since a titration experiment is performed in which L is titrated into a solution of M (or M into a solution of L), K_A and the stoichiometry, n, of the complex are also obtained by ITC. Moreover, ITC experiments performed at different temperatures yield ΔC_p defined by Eq. (3).

[1] In this article the components of a complex are designated L and M, irrespective of their size and chemical nature. Thus, L and M can be proteins, nucleic acids, low molecular weight metabolites, salt ions, and so on. L often is named the ligand and M the receptor. However, this assignment is arbitrary.

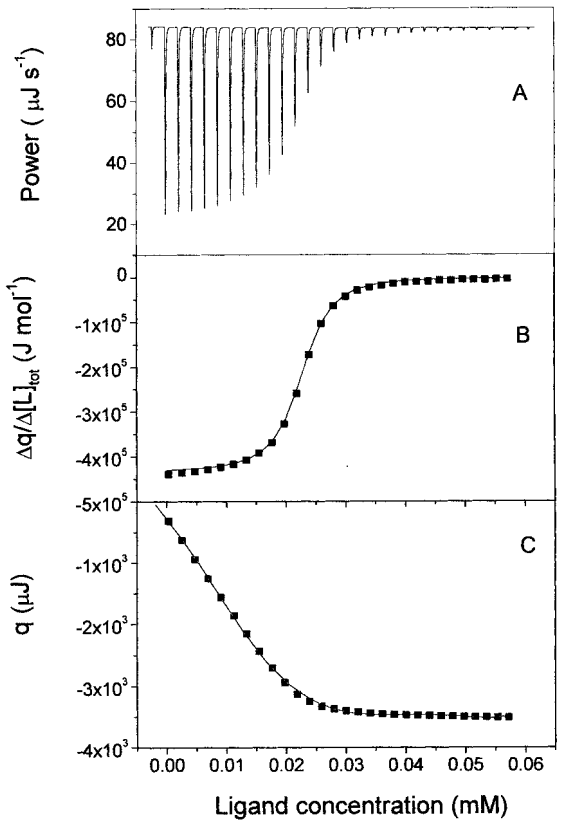

Figure 1. ITC titration data describing the formation of a 16 bp DNA duplex by mixing the complementary strands at 30 °C. *Panel A* shows the differential power signal recorded in the experiment. After integration with respect to time and normalization per mol of added ligand (which in this case is single-stranded DNA), ΔH_{app}, K_A and n can be calculated from Eq. (6) by nonlinear least squares analysis, as detailed in the text. The integrated data can be plotted in two ways: as a sigmoidal plot (*panel B*) or as a hyperbolic saturation curve (*panel C*). The ΔH_{app} obtained from this analysis is a global property of the system corrected for nonspecific effects. The solid lines in panels B and C correspond to $\Delta H_{app} = 436$ kJ mol^{-1}, $K_A = 3.1 \times 10^6$M^{-1}, and $n = 1$.

The ITC experiment

The basic principle is simple.[2] The experiment is performed at a constant temperature by titrating one binding partner (called the 'titrant', e.g. *L*) into a solution containing the other binding partner (called the 'titrand', e. g. *M*) in the sample cell of the calorimeter. After each addition of a small aliquot of *L*, the heat released or absorbed in the sample cell is measured with respect to a reference cell filled with buffer. The heat change is expressed as the electrical power (J s^{-1}) required to maintain a constant small temperature difference between the sample cell and the reference cell, which are both placed in an adiabatic jacket. Addition of *L* is automated and occurs from a precision syringe driven by a computer-controlled stepper motor. The contents of the sample cell are stirred to effect rapid mixing of the reactants. In commercially available instruments volumes of sample cells are in the range 0.2–1.4 ml. The amount of titrand required per experiment depends on the magnitude of the heat change; 10–100 nmol of protein are typical.

Figure 1A shows the raw data of an ITC experiment. Each peak corresponds to the heat released on addition of an aliquot of ligand to the receptor. Integration of the differential power signal with respect to time yields the apparent heat change, $\Delta q_{i,app}$, between additions $i-1$ and i:

$$\Delta q_{i,app} = q_i - q_{i-1}$$

$\Delta q_{i,app}$ corresponds to the area of the ith peak in Fig. 1A. If K_A is large and the molar ratio of *L* to *M* at the beginning of the titration is low, then virtually all the ligand is bound to the receptor and the peak areas are similar. As the fractional saturation increases, $\Delta q_{i,app}$ gradually decreases. Eventually all receptor sites are saturated. Small heat changes registered after full saturation are caused by the heat of ligand dilution, $q_{i,dil}$, and by other nonspecific effects, $q_{i,ns}$. $\Delta q_{i,app}$ is proportional to the volume of the calorimetric cell, V_{cell}, to the change in concentration of the bound ligand, $\Delta[L_i]_{bound} = [L_i]_{bound}, - [L_{i-1}]_{bound}$, and to the apparent molar enthalpy of association, ΔH_{app}. We write:

$$\begin{aligned}\Delta q_{i,app} &= \Delta q_i + \Delta q_{i,dil} + \Delta q_{i,ns} \\ &= \Delta[L_i]_{bound} \times V_{cell} \times \Delta H_{app}\end{aligned} \quad (6a)$$

$\Delta q_{i,dil} + \Delta q_{i,ns}$ is obtained from a blank titration of ligand into buffer. V_{cell} is known, and ΔH_{app} is constant at fixed pressure, temperature and solvent conditions. ΔH_{app} and K_A are calculated from:

$$\Delta q_i = \Delta q_{i,app} - \Delta q_{i,dil} - \Delta q_{i,ns} = n[M]_{tot} V_{cell} \Delta H_{app} \times \mathbb{R} \quad (6b)$$

$[M]_{tot}$ is the total concentration of *M* in the sample cell of the calorimeter. Δq_i is the effective heat change caused by the formation of complex *ML* at the ith step of the titration, and $\mathbb{R}$ is the root of the quadratic equation:

$$Y_i^2 - Y_i \times \left(1 + \frac{1}{nK_A[M]_{tot}} + \frac{[L_i]_{tot}}{n[M]_{tot}}\right) + n[L_i]_{tot}[M]_{tot} = 0 \quad (7)$$

Y_i is the degree of saturation defined by $Y_i = \Delta[L_i]_{bound}/[M]_{tot}$. $[L_i]_{tot}$ is the total concentration of *L* added until injection *i*, and *n* is the number of identical and independent binding sites for the ligand *L* on the receptor *M*. A nonlinear regression procedure based on Eq (6b) yields *n*, K_A and ΔH_{app} from a single titration experiment.

The experimental data can be plotted in two ways. In the differential mode the total heat accumulated up to injection *i* is normalized to the total ligand concentration at step *i* and is plotted against the total ligand concentration at step *i* (or against the ratio of the total ligand concentration at step *i* to the total receptor concentration, $[L_i]_{tot}/[M]_{tot}$). This yields the familiar sigmoidal titration curve shown in Fig. 1B from which the total calorimetric heat change per mol of complex, ΔH_{app}, can be calculated. In the integral mode, the total cumulative heat is plotted against the total ligand concentration to yield a hyperbolic saturation curve (Fig.

[2] Technical details on the construction of modern mixing calorimeters, their performance and sensitivity, and on the theory of data analysis have been described elsewhere (McKinnon *et al.*, 1984; Wiseman *et al.*, 1989; Freire *et al.*, 1990; Breslauer *et al.*, 1992).

1C). The same parameters are obtained from either plot. Comparative statistical analysis of the two plots can give information about the accumulation of systematic errors (Bundle and Sigurskjold, 1994). The number of binding sites, n, and ΔH_{app} are strongly correlated, and the successful deconvolution of the binding isotherm often depends on additional independent information about the number of binding sites of M.

The case discussed applies only to the binding of L to a receptor M with n identical and independent binding sites. In the case of a receptor with multiple binding sites of different affinity, statistical thermodynamic treatment of the data is required. The partition function Q gives a general description of a binding reaction (Wyman and Gill, 1990). Q relates the sum of concentrations of all species to the concentration of an arbitrarily chosen reference species, conveniently the unligated form of a receptor:

$$Q = \frac{[M] + \sum_{j=1}^{n}[ML_j]}{[M]} = 1 + \frac{\sum_{j=1}^{n}[ML_j]}{[M]} = 1 + \sum_{j=1}^{n}\beta_j \cdot [L]^j \tag{8}$$

In this equation, $[L]$ and $[ML_j]$ are the concentrations of free ligand and ligated receptor, respectively, n is the number of binding sites on the receptor, and β_j is the overall binding constant relative to the unligated receptor. It can be written in terms of the overall step-wise (macroscopic) binding constants, K, as

$$\beta_j = \prod_{j=1}^{n} K_j$$

or in terms of the intrinsic (microscopic) site binding constants, κ, as

$$\beta_j = \frac{n!}{j!(n-j)!}\prod_{j=1}^{n}\kappa_j$$

Different binding models can be discriminated depending on the definition of β_j. In the case of a single binding site, Eq. (8) reduces to:

$$Q = 1 + K_A[L] \tag{8a}$$

where K_A is the intrinsic (microscopic) site binding constant. If the receptor has one set of j identical and independent binding sites:

$$Q = (1 + K_A \cdot [L])^j \tag{8b}$$

For m sets, each containing j identical and independent binding sites:

$$Q = \prod_{1}^{m}(1 + K_{A,m} \cdot [L])^{j_m} \tag{8c}$$

In the case of cooperativity between *a priori* identical binding sites, the first ligand binds with $K_{A,1} = K_A$, the second with $K_{A,2} = a \times K_A$, the third with $K_{A,3} = a \times b \times K_A$, and so on. The cooperativity factors a, b, … account for the change of intrinsic binding affinity of the unoccupied sites when the degree of saturation increases.

Equation (7) shows that the deconvolution of the binding isotherm from an ITC experiment requires calculation of the change in the degree of saturation, Y_i, with ligand concentration. In terms of the binding partition function, Y_i is expressed by

$$Y_i = \frac{\partial \ln Q}{\partial \ln[L]} = \frac{\sum_{j=1}^{n} j\beta_j[L_i]^j}{Q} \tag{9}$$

Since $[L_i]_B = [M]_{tot} \times Y_i$, the total heat change after completion of injection i is

$$\Delta q_i = M_T \times V_{cell}\frac{\sum_{j=1}^{n}\Delta H_{app,i}\, j\beta_j[L_i]^j}{Q} \tag{10}$$

With the help of this statistical thermodynamic treatment it is possible to deconvolute a heat binding isotherm of a complex system involving non-equivalent and/or interacting binding sites. There are instructive examples demonstrating the strength of this approach (Eisenstein *et al.*, 1994; Ferrari and Lohman, 1994; Hyre and Spicer, 1995; Bruzzese and Connelly, 1997; Gopal *et al.*, 1997). The deconvolution has a firm thermodynamic foundation and avoids additional assumptions as is necessary in the analysis of spectroscopic binding data. In practice, however, the success much depends on the quality of the experimental data and on the number of coupled fitting parameters.

Informational content of ITC data

Free energy changes. As in other binding experiments, to obtain reliable binding constants the concentrations of the interacting species have to be in a proper range so that both the free ligands and the complex are populated. If the concentration of binding sites is very much higher than $1/K_A$, all the ligand added will be bound until saturation, and the binding isotherm as displayed in Fig. 1B has a rectangular shape with a slope approaching infinity. In the opposite case in which the binding site concentration is much below $1/K_A$, the binding isotherm is very shallow and full saturation is difficult to approach. For accurate values of K_A, the concentration of receptor binding sites should not be very much higher than $1/K_A$. The dimensionless number obtained by multiplying K_A with the total binding site concentration is called the c-value (Wiseman *et al.*, 1989). As a rule of thumb, c-values between 10 and 100 give good K_A-values. Often, however, optimal concentrations are not accessible. For very tight binding reactions, optimal concentrations are too small to yield measurable heat changes. It is for this reason that even with the most sensitive instruments presently available, K_A higher than about 10^9 M^{-1} ($\Delta G \sim -50$ kJ mol^{-1} at room temperature) can not be very accurately measured. Very tight binding can be analyzed by DSC to be discussed in the section Differential Scanning Calorimetry. At the other extreme when K_A is very low, the concentrations required for c-values between 10 and 100 may be so high that aggregation of macromolecules can obscure the binding reaction.

If ΔG of binding is temperature dependent, it is sometimes possible to chose a temperature at which K_A can be measured by ITC. Unfortunately, often K_A is practically independent of temperature because of strong enthalpy/entropy compensation. In this case, the thermodynamic linkage theory provides a general framework for calculating high binding constants from an appropriate thermodynamic cycle. For example, K_A can change with pH and one may chose a pH where K_A can be obtained by ITC. If the pK_a values of the ligated and the ligand-free form of the receptor is known, ΔG at the tight binding pH conditions can be calculated (Doyle *et al*., 1995; Baker and Murphy, 1996; Kavanoor and Eftink, 1997). Alternatively, ITC titrations can be conducted by titrating a strongly binding ligand into a solution containing the receptor already saturated with a weaker ligand. Free binding energies are obtained from such a displacement experiment if the strong and weak ligands exhibit suitable differences in binding enthalpy (Khalifah *et al*., 1993; Hu and Eftink, 1994; Sigurskjold *et al*., 1994).

Enthalpy changes. The molar binding enthalpy ΔH_{app} is a fitting parameter according to Eqs (6b) and (10) and is obtained together with K_A from data collected in the optimal concentration range. A better practice is to measure ΔH_{app} at concentrations where the binding partners are fully associated when the degree of saturation is still low. In such experiments the accuracy of ΔH_{app} is better, yet the *c*-value is too high for accurate determination of K_A. Thus, in practice K_A and ΔH_{app} are best obtained from experiments performed at different concentration ratios.

The enthalpy change measured by ITC is a global property of the whole system. It is the *total* heat released or absorbed in the calorimetric cell on each addition of the ligand. The total heat contains contributions arising from nonspecific effects. These are the heat of dilution of the ligand into buffer, heat caused by the incomplete match of the temperatures of the solutions in the cell and at the injection syringe tip, or heat effects from mixing of buffers of slightly different chemical composition. The nonspecific heat effects are accounted for by $\Delta q_{i,dil}$ and $\Delta q_{i,ns}$ in Eqs (6a) and (6b). But even the corrected heat change Δq_i of Eq. (6b) is itself composed of different contributions. This is the reason why the molar enthalpy change is an *apparent* quantity (ΔH_{app}). It only depends on the initial and final state of the binding reaction, the solvated free molecules and the final solvated complex.

Contribution of reorganization of solvent to ΔH_{app} *and* ΔG. From the comparison of the calorimetric enthalpy change in H_2O and D_2O it was concluded that solvent reorganization accounts for a large portion of ΔH_{app} (Connelly *et al*., 1993; Chervenak and Toone, 1994). Indeed, in high-resolution crystal structures, water molecules can be seen at the complex interface where they may improve the complementarity of the interacting surfaces, and bound water is sometimes visible at the empty contact surface of the free molecules (Ladbury, 1996). Extended H-bond networks at the complex interface can make the enthalpy change more favorable, often counterbalanced by an entropic penalty (Bhat *et al*., 1994; Holdgate *et al*., 1997). That addition or removal of interfacial water contributes to the free energy of binding was directly shown by lowering the water activity through addition of glycerol or another osmolyte (Kornblatt *et al.*, 1993; Robinson and Sligar, 1993; Jelesarov and Bosshard, 1994; Goldbaum *et al.*, 1996; Xavier *et al.*, 1997). Complexes with a low degree of surface complementarity and with no net change of hydration are tolerant to osmotic pressure (Lundbäck *et al*., 1998).

Contribution of direct noncovalent bonds to ΔH_{app}. Apart from the bulk hydration effects, direct noncovalent bonds at the interface contribute to ΔH_{app}. These contributions may be considered to represent the binding enthalpy in a strict sense. Yet it is very difficult to sort out the enthalpy of formation of each specific noncovalent interaction. The net enthalpy effect of a particular noncovalent bond *X–Y* at the interface can result from the balance between the interaction enthalpy of the bond *X–Y* in the complex and the enthalpies from bonds between the solvent or solutes and *X* and *Y* in the isolated molecules. Further, subtle rearrangements of the packing interactions at the binding site compared to the free molecule may add to ΔH_{app}.

Mutational approaches have been tried to analyze the contributions of individual bonds to the enthalpy change. Examples are alanine scanning mutagenesis (Pearce *et al*., 1996), removal of a particular H-bond at the binding site (Connelly *et al.*, 1994), or the construction of double mutant cycles (Frisch *et al.*, 1997). Calorimetric analysis of mutants suffers from a major problem: Can one attribute a change of ΔH_{app} to the removal of a specific contact? Or is the enthalpic effect of an indirect nature and decomposition of ΔH_{app} in terms of individual residue-residue contacts or even atom-atom interactions is not possible? It has been argued on theoretical grounds that such decomposition of ΔH_{app} (as well as of ΔG and ΔS) is not possible (Mark and van Gunsteren, 1994). But others have argued in favor of decomposition of ΔH_{app} (Boresch and Karplus, 1995; Brady and Sharp, 1995).

In general, changes of ΔH_{app} are not, or only weakly correlated to changes in ΔG. Recent careful analysis of three protein systems indeed suggests the correlation can not be made (Ito *et al.*, 1993; Pearce *et al.*, 1996; Frisch *et al.*, 1997). One reason for this unfortunate situation is enthalpy/entropy compensation. The overall change in binding enthalpy due to a particular mutation can be partly compensated by an entropy change. As a result, there only is a small change in the free energy of binding. This common thermodynamic behavior is thought to reflect a major role of compensating enthalpy and entropy contributions of water to the binding process (Lumry and Rajender, 1970; Dunitz, 1995; van Oss, 1997).

Calorimteric and van't Hoff enthalpy changes. The van't Hoff enthalpy change (ΔH_{vH}) is calculated from the temperature dependence of K_A obtained either by ITC or calculated from spectroscopic or other data [Eq. (5)]. Hence, ΔH_{vH} reflects the enthalpy intimately associated with the binding event that causes the signal change, for example the quenching of the fluorescence of a tryptophan residue in the complex *ML*. Therefore, ΔH_{vH} equals ΔH_{cal} only if the binding reaction follows a two-state transition between free and bound molecules and if the signal change used to calculate K_A reflects the entire population of free and bound molecules. Otherwise, ΔH_{cal} and ΔH_{vH} are different. Indeed, systematic discrepancies between ΔH_{cal} and ΔH_{vH}

have been reported (Gilli *et al.*, 1994; Naghibi *et al.*, 1995) and there have been attempts to rationalize the differences (Dunitz, 1995; Chaires, 1997; van Oss, 1997). On the other hand, a ratio of $\Delta H_{cal}/\Delta H_{vH} = 1$ can be taken to indicate that a binding event conforms to a two-state transition from free molecules to the complex with no detectable intermediates and with at most very minor contributions from water reorganization, conformational rearrangements, or changes in the state of protonation.[3]

Protonation effects. Among the many possible contributions to ΔH_{app}, the effect of changes in the protonation state is worth considering in more detail because the number of protons, n_{H+}, taken up or released during the binding process can be measured by titration calorimetry (Murphy *et al.*, 1993; Jelesarov and Bosshard, 1994; Gomez and Freire, 1995; Kresheck *et al.*, 1995). If binding involves a change in the protonation state of *L* and/or *M*, protons are exchanged with the buffered medium. Therefore, the calorimetrically observed enthalpy change, ΔH_{app}, depends on the enthalpy of ionization of the buffer, ΔH_{buffer}. Repeating the experiment at the same pH in buffers of different ΔH_{buffer} allows one to calculate the binding enthalpy, ΔH_{bind}, from:

$$\Delta H_{app} = \Delta H_{bind} + n_{H+} \times \Delta H_{buffer} \qquad (11)$$

Values of ΔH_{buffer} have been tabulated (Christensen *et al.*, 1976) or can be measured by ITC (Jelesarov and Bosshard, 1994). ΔH_{bind} can be partitioned further into a term that is independent of the protonation change, $\Delta H'_{bind}$, and a term describing the enthalpic contribution of the protonation reaction, ΔH_{H+}:

$$\Delta H_{bind} = \Delta H'_{bind} + n_{H+}\Delta H_{H+} \qquad (11a)$$

Combining Eqs (11) and (11a):

$$\Delta H_{app} = \Delta H'_{bind} + n_{H+}(\Delta H_{H+} + \Delta H_{buffer}) \qquad (11b)$$

If a pH can be found where binding is pH-independent ($n_{H+} = 0$), $\Delta H_{app} = \Delta H'_{bind}$ follows from Eq. (11b). Figure 2 shows an example in which binding of two proteins is accompanied by the uptake of a single proton. This system was particularly revealing since $\Delta H'_{bind}$ was 26kJ mol^{-1}, very much higher than ΔH_{app} because $\Delta H'_{bind}$ and ΔH_{buffer} almost canceled at pH 7. In practice, it is recommended to always repeat the ITC experiment at the same pH in a buffer that has a different heat of ionization. If the same ΔH_{app} is found in both buffers, there is no change in protonation of *L* and/or *M* when the complex forms. Conversely, variation of ΔH_{app} with buffer is a clear sign of a protonation event during the association reaction. Occasionally, one may obtain a hint from ΔH_{H+} (deduced with the help of Eq. 11) about the nature of the group(s) undergoing protonation/deprotonation (Jelesarov and Bosshard, 1994; Gomez and Freire, 1995; Baker and Murphy, 1997).

Heat capacity changes. Modern ITC instruments allow to precisely measure ΔH_{app} between about 5 and 70°C, and ΔC_p can be calculated from a plot of ΔH_{app} *versus* *T* (Eq. 3). In many cases such plots are linear within the experimental error in a narrow temperature range, suggesting that ΔC_p itself does not depend on temperature. What is the origin of the change in heat capacity when a complex is formed? ΔC_p is almost always negative if the complex is taken as the reference state. This means that the complex has a smaller heat capacity than the sum of its free components. This and other observations as well as theoretical considerations indicate that ΔC_p originates from changes in the degree of surface hydration in the free and the complexed molecules, and to a lesser extent also from changes in molecular vibrations (Sturtevant, 1977; Murphy and Freire, 1992; Spolar *et al.*, 1992; Gomez *et al.*, 1995; Makhatadze and Privalov, 1995). The often seen temperature-independence of ΔC_p infers that neither the area of contact surface nor the difference of the vibrational content between the complex and its components change within the observed temperature range.

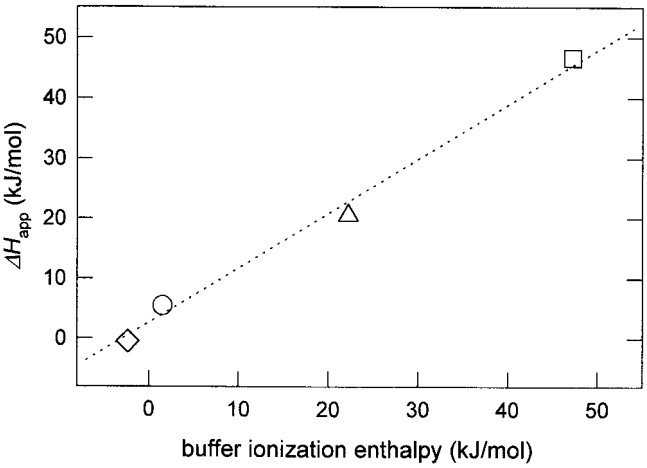

Figure 2. Apparent enthalpy change, ΔH_{app}, for the binding of ferredoxin to ferredoxin:NADP$^+$ oxidoreductase at 27°C as a function of the ionization enthalpy of the buffer. ITC experiments were performed at pH 7.5 in Tris (square), Mops (triangle), phosphate (circle), and cacodylate buffer (diamond). Dashed line: linear least squares fit to Eq. (11). Slope = 0.96 ± 0.03; intercept at zero buffer ionization enthalpy = 1.03 ± 1.46 kJ mol^{-1}. (Adapted from Jelesarov and Bosshard, 1994.)

Calculated and measured ΔC_p. The association of two proteins to a complex can be compared to the folding of a single protein. In both reactions a substantial fraction of polar and nonpolar surface is buried and the degree of surface hydration is likely to change. There are semi-empirical methods to calculate ΔC_p from the change of the water-accessible polar and nonpolar surface area in protein folding and in protein association (Murphy and Freire, 1992; Spolar *et al.*, 1992; Makhatadze and Privalov, 1995). Several communications report good agreement between the experimentally determined ΔC_p and that calculated from the molecular surface buried in the complex (Connelly and Thomson, 1992; Murphy *et al.*, 1993; Baker and Murphy, 1997; McNemar *et al.*, 1997). However, a good correlation seems to hold only for those interactions that conform to a lock-and-key or rigid-body binding model. Very often this

[3] For $\Delta H_{cal}/\Delta H_{vH} = 1$ in a system in which there is considerable water reorganization, conformational rearrangement or change in protonation states, the observable p_i of Eq. (4) has to mirror all the above phenomena. This seems not very likely in case the observable is, for example, a fluorescence change of a single chromophore.

model is inadequate. Significant discrepancies between calculated and measured ΔC_p were reported for small ligand binding (Faergeman *et al.*, 1996; Holdgate *et al.*, 1997), for protein-protein complexes (Bhat *et al.*, 1994; Pearce *et al.*, 1996), and most notably for protein-DNA complexes (Jin *et al.*, 1993; Ladbury *et al.*, 1994; Ayala *et al.*, 1995; Merabet and Ackers, 1995; Berger *et al.*, 1996; Oda *et al.*, 1998). It is accepted that a lack of correlation between measured and calculated values of ΔC_p is a consequence of folding transitions coupled to the association event (Spolar and Record, 1994), and also to significant dynamic restriction of vibrational modes at the complex interface (Botuyan *et al.*, 1993; Ladbury *et al.*, 1994; Berglund *et al.*, 1997). Interestingly, weaker complexes tend to show larger ΔC_p values per unit of surface area of contact. The likely reason is enhanced enthalpic and entropic fluctuation at a less tight complex interface (Tidor and Karplus, 1994). Large conformational rearrangements during binding and the preexistence of temperature-dependent conformational equilibria can cause deviations from linearity in the plots of ΔH_{app} against T, that is, temperature-dependent ΔC_p (Ferrari and Lohman, 1994; Bruzzese and Connelly, 1997). No doubt, the methods to calculate ΔC_p from the parametrization of structural data need much improvement before becoming reliable predictors of heat capacity changes. In the meantime one has to rely on experiments. Here, a very careful examination of the conformational states of the molecules in isolation and of the complex they form is required to account for the observed energetic values in structural terms (Pearce *et al.*, 1996; Wintrode and Privalov, 1997; Oda *et al.*, 1998). This information can be obtained by DSC.

Entropy changes. The entropy of association can be calculated from measured values of ΔG, ΔH and ΔC_p according to the laws of thermodynamics. The change in entropy of a complex relative to the unligated molecules is largely caused by hydration effects because the entropy of hydration of polar and apolar groups is large and there is significant reduction of water accessible surface on binding. Therefore, when a complex is formed the overall entropy change is often large and often positive. Occasionally, however, ordering of water at the complex interface occurs, which contributes unfavorably to ΔS and favorably to ΔH (Holdgate *et al.*, 1997). Another important, unfavorable contribution to the entropy change originates from the reduction of side chain mobility at the binding site. Furthermore, a statistical term has to be added to the entropy change to account for the reduction in the number of particles and their degrees of freedom in the complex. Different estimates of the mixing entropy have been discussed, yet it appears that the 'cratic' correction accounts adequately for the loss of translation and rotation (Kauzmann, 1959; Murphy *et al.*, 1994; Tamura and Privalov, 1997). Obviously, a negative entropy change can have different reasons and, most importantly, does not necessarily indicate that hydration of the interface remains unchanged or increases with respect to the free complex partners. On the other hand, a positive ΔS is a strong indication that water molecules have been expelled from the complex interface.

Concluding remarks on ITC

The beauty of titration calorimetry is in its simplicity, which allows to obtain the entire set of thermodynamic parameters from performing only a few experiments at a series of different temperatures. The difficulty, however, lies in the fact that the observed heat change, which is the immediate outcome of ITC, is a global property. Only in those cases where the binding reaction follows a lock-and-key or rigid-body mechanism that can be described by a two-state transition between free and complexed molecules, and in which there is no change in the protonation state of L and/or M nor in the hydration state of the interface, ΔH_{app} is equal to the 'true' binding enthalpy attributable to noncovalent bonds in the complex. A good indicator – though no proof – for this simple mechanism is the equality $\Delta H_{cal} = \Delta H_{vH}$. In the majority of cases ΔH_{app} has different origins, which often are difficult to distinguish. The contributions to ΔH_{app} sometimes can be separated. For example, a positive entropy change is a good indication for the extrusion of water from the complex interface. A change of ΔH_{app} with the chemical nature of the buffer points to a protonation/deprotonation event concurrent with the binding reaction, and careful analysis of ΔH_{app} with buffer and pH can reveal the number and sometime even the nature of the group(s) whose ionization state changes. Finally, calculation of ΔC_p from the area of the surface buried in the complex (possible only if the necessary three-dimensional structures are available) and comparison with ΔC_p obtained by ITC can give a clue as to changes in conformational states and vibrational contents between the complex and its free components. These latter changes can be analyzed in more detail with the help of DSC to be discussed now.

Differential Scanning Calorimetry

DSC is the most direct experimental technique to resolve the energetics of conformational transitions of biological macromolecules. By measuring the temperature dependence of the partial heat capacity, a basic thermodynamic property, DSC gives immediate access to the thermodynamic mechanism that governs a conformational equilibrium, for example between the folded and the unfolded forms of a protein, or between single and double stranded DNA. The theory of DSC and the thermodynamic interpretation of the experimental data have been the subject of excellent reviews (Privalov and Potekhin, 1986; Sturtevant, 1987; Freire, 1995). The combination of DSC with ITC to characterize the energy profile of an interacting system in a broad temperature interval and at varying solvent conditions has been brought up before (Connelly, 1994; Plum and Breslauer, 1995). Here we wish to give a basic description of the informational content of DSC measurements with special emphasis on the potential of DSC to analyze the energetics of macromolecular association reactions.

The DSC experiment

DSC measures the heat capacity of a solution of the

molecule under study as a function of temperature. Modern scanning calorimeters are equipped with twin cells and operate in a differential mode. The solution containing the solute – in the present context a biological macromolecule – is placed in the sample cell and an equal volume of solvent (buffer) in the reference cell. The system is heated (or cooled) quasi-adiabatically at a constant rate, typically 0.5–1.5 K min^{-1}. [4] Since the heat capacities of the solution in the sample cell and the solvent in the reference cell differ, a certain amount of electrical power is required to zero the temperature difference between the two cells. The power difference (J s^{-1}), after normalization by the scanning rate (K s^{-1}), is a direct measure of the heat capacity difference between the solution and the solvent: $\Delta C_p^{\text{sol-solv}} = C_p^{\text{sol}} - C_p^{\text{solv}}$ (in units of J K^{-1}).

Obviously, one is interested in C_p(T), the *partial specific heat capacity* (J K^{-1} g^{-1}) of the solute *M* To obtain C_p(T), the partial specific heat capacity of the solvent, $C_{p,solv}$(T), has to be subtracted. This correction requires precise knowledge of the masses of the macromolecule and the solvent, of the mass of the solvent displaced by the macromolecule, and of the partial specific volumes of the macromolecule and the solvent. These quantities are temperature dependent and the coefficients of thermal expansion of the chemical species as well as of the calorimetric cell must be known. It can be shown that the partial specific heat capacity of the solute *M* (in units of J K^{-1} g^{-1}) is given by:

$$C_p(T) = C_p^{\text{solv}} \frac{\bar{v}_M}{\bar{v}_S} + \frac{\Delta C_p^{\text{sol-solv}}}{m_M} \qquad (12)$$

m_M and $\bar{v}_M$ are, respectively, the mass and the partial specific volume of *M*, and $\bar{v}_s$ is the partial specific volume of the solvent.

Because the measured power difference, $\Delta C_p^{\text{sol-solv}}$, is small and the volumes of the calorimetric cells are 0.3–1.5 ml, milligram amounts of biomacromolecules are necessary for DSC measurements. In some cases, the macromolecule concentrations may be so high that the solutions are far from the ideal condition to which the thermodynamic models apply. This difficulty has to be kept in mind when performing DSC measurements and one has to check for nonspecific aggregation of macromolecules in the calorimeter cell, often revealed by a faint turbidity when the solution is removed from the cell after the experiment.

Informational content of DSC data

The first result obtained from a DSC experiment is the partial specific heat capacity, $C_p(T)$. This quantity contains important information about the conformational state of a protein in the temperature interval of the experiment. For small globular proteins, the absolute value of C_p at 25 °C varies in the range 1.2–2.3 J K^{-1} g^{-1} and increases linearly with temperature with a slope of (6–8) $\times 10^{-3}$ J K^{-2} g^{-1}. Deviations from these values may indicate loose packing of the protein or structural fluctuations (Privalov and Potekhin, 1986; Gomez *et al.*, 1995). The partial specific heat capacity of the native protein is significantly lower than that of the denatured protein. C_p of a fully unfolded protein can be approximated from the amino acid sequence by summing up the heat capacities of the amino acid residues and the contributions of the peptide bonds (Privalov and Makhatadze, 1990; Makhatadze and Privalov, 1995). If the experimentally measured C_p after completion of unfolding is lower than C_p calculated from the amino acid sequence, this may indicate that the denatured protein has some residual structure and is not a fully solvated polypeptide chain.[5]

When a protein solution is heated up, C_p(T) follows a peak-shaped curve if protein denaturation is cooperative and reversible. Figure 3 shows a typical DSC trace, also called a thermogram or a thermal transition curve. The protein denatures in the temperature interval T_1 to T_2 with a transition midpoint T_m.

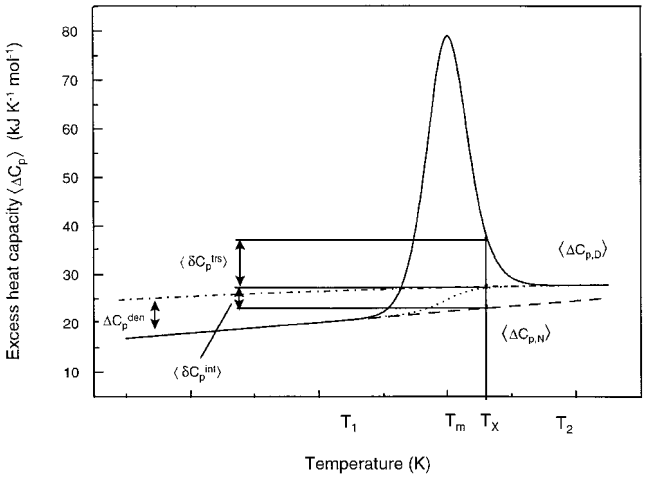

Figure 3. Partial molar heat capacity of a protein undergoing reversible thermal denaturation in the temperature interval T_1–T_2 and with a transition midpoint at T_m. The heat capacity of the native state, $\langle C_{p,N} \rangle$, shows a linear temperature dependence (dashed line). The heat capacity of the denatured state, $\langle C_{p,D} \rangle$, is approximated by a quadratic function (dashed-dotted line). The functions $\langle C_{p,N}(T) \rangle$ and $\langle C_{p,D}(T) \rangle$ can be extrapolated into the transition zone between T_1 and T_2 in proportion to the progress of transition (dotted line). The difference between $\langle C_{p,D} \rangle$ and $\langle C_{p,N} \rangle$ is the heat capacity increment of protein denaturation, ΔC_p^{den}. It is positive because the denatured protein has a larger heat capacity than the native protein. The excess partial heat capacity, $\langle \Delta C_p \rangle$, is defined as $\langle \Delta C_p \rangle = \langle C_p \rangle - \langle C_{p,N} \rangle$. $\langle \Delta C_p \rangle$ is composed of the intrinsic excess heat capacity, $\langle \delta C_p^{int} \rangle$, which accounts for all the molecular species that become populated in the progress of the transition from the native to the denatured state, and from the transition excess heat capacity, $\langle \delta C_p^{trs} \rangle$, originating from the increased fluctuation of the system when the protein changes between different enthalpic states in the course of thermal denaturation. The relative magnitudes of $\langle \delta C_p^{int} \rangle$ and $\langle \delta C_p^{trs} \rangle$ at temperature T_x are indicated.

[4] A constant pressure is applied to the two cells. Depending on this pressure, the upper temperature limit can be as high as 150 °C for aqueous solutions.

[5] The term 'denatured' refers to the ensemble of conformational states when thermal transition is complete. In practice, this is at a temperature well above the transition temperature T_m. The denatured protein is not necessarily equivalent to the completely unfolded protein, which is an idealized state referring to the polypeptide chain in its fully solvated conformation. Here we prefer the term 'denatured' to indicate this difference.

For a meaningful comparison of the thermal transition curves of different substances the specific heat capacity is inadequate because it is normalized to the mass of substance. The appropriate quantity is the partial *molar* heat capacity, $\langle C_p \rangle$, which has units of J K^{-1} mol^{-1}. It is obtained by multiplying C_p (J K^{-1} g^{-1}) by the molecular weight (g mol^{-1}). The angular brackets, $\langle\ \rangle$, designate the ensemble-averaged population of all molecular states that become populated during the transition from the native to the denatured form. It is very important to recognize that during the transition the partial heat capacity function can no longer be ascribed to a single structural state.

The partial molar heat capacity of the native protein, $\langle C_{p,N} \rangle$, can be approximated by a linear function (dashed line in Fig. 3), and that of the denatured protein, $\langle C_{p,D} \rangle$, by a quadratic function (dash-dotted line in Fig. 3) (Griko *et al.*, 1994b; Viguera *et al.*, 1994; Xie *et al.*, 1994). The *heat capacity increment* accompanying protein denaturation, or heat capacity of denaturation for short, is defined as $\Delta C_p^{den} = \langle C_{p,D}(T) \rangle - \langle C_{p,N}(T) \rangle$. It is positive because the denatured protein has a larger heat capacity than the native protein. The absolute specific ΔC_p^{den} is similar for many globular proteins, typically 0.3 to 0.7 J K^{-1} g^{-1}. A positive ΔC_p^{den} is mainly a consequence of hydration effects dominated by the positive heat capacity of hydration of apolar groups, which become exposed to the solvent water after disruption of the compact folded conformation. Semi-empirical methods have been developed correlating ΔC_p^{den} with the increase of solvent accessible surface upon denaturation (Murphy and Freire, 1992; Spolar *et al.*, 1992; Makhatadze and Privalov, 1995).[6]

Excess heat capacity, excess enthalpy and excess entropy. If the native state is taken as a reference, an *excess partial molar heat capacity* can be defined as

$$\langle \Delta C_p \rangle = \langle C_p \rangle - \langle C_{p,N} \rangle$$

The excess heat capacity can be divided in two components. The first component accounts for the sum of the molecular species that become populated in the progress of the transition from the native to the denatured state.[7] This component is often referred to as the *intrinsic* excess heat capacity, $\langle \delta C_p^{int} \rangle$. The second contribution to $\langle \Delta C_p \rangle$ originates from the increased fluctuation of the system when the protein changes between different enthalpic states in the course of thermal denaturation. This component is called *transition* excess heat capacity, $\langle \delta C_p^{trs} \rangle$, and is usually much larger than $\langle \delta C_p^{int} \rangle$ as indicated in Fig. 3. The excess molar heat capacity can now be written as:

$$\langle \Delta C_p \rangle = \langle \delta C_p^{int} \rangle + \langle \delta C_p^{trs} \rangle \qquad (13)$$

To calculate $\langle \delta C_p^{int} \rangle$, the functions $\langle C_{p,N}(T) \rangle$ and $\langle C_{p,D}(T) \rangle$ have to be extrapolated into the transition zone between T_1 and T_2 in proportion to the progress of transition (Sturtevant, 1987). This extrapolation is indicated by the dotted line in Fig. 3. The excess enthalpy of the thermal denaturation, ΔH_{den}, is defined by:

$$\Delta H_{den} = \int_{T_1}^{T_2} \langle \delta C_p^{trs} \rangle \mathrm{d}T \qquad (14)$$

ΔH_{den} corresponds to the area of the peak above the dotted line in Fig. 3. The excess entropy of denaturation is defined by:

$$\Delta S_{den} = \int_{T_1}^{T_2} \frac{\langle \delta C_p^{trs} \rangle}{T} \mathrm{d}T \qquad (15)$$

ΔH_{den} represents the 'true' calorimetric estimate of the denaturation enthalpy and is a model-independent value, i.e. it does not depend on the shape of the transition curve between T_1 and T_2.

The integral of δC_p^{trs} [Eq. (14)] can also be analyzed according to the van't Hoff equation to obtain ΔH_{den}^{vH}, sometimes called the 'effective' enthalpy of transition. ΔH_{den}^{vH} is model-dependent. The reason is that determination of ΔH_{den}^{vH} assumes an equilibrium between only two forms, native and denatured protein, to calculate an equilibrium constant $K(T)$ from which ΔH_{den}^{vH} follows according to Eq. (5a). ΔH_{den}^{vH} now can be compared with the calorimetric, model-independent enthalpy change, ΔH_{den}^{cal}, described by Eq. (14) (the superscript^{cal} is added only to distinguish the calorimetrically measured quantity from the calculated van't Hoff enthalpy change). If $\Delta H_{den}^{vH} / \Delta H_{den}^{cal} = 1$, denaturation is thought to obey a two-state, cooperative unfolding reaction. A ratio >1 may indicate significantly populated intermediate states. Values above unity also result if the definition of the cooperatively folding unit is not the same in the calorimetric and in the van't Hoff analysis. This is the case if the excess heat capacity function does not display a symmetric curve and hides transitions between more than two states.[8] A ratio <1 points to an irreversible process. The approach to compare ΔH_{den}^{vH} with ΔH_{den}^{cal}, both calculated from DSC data as outlined above, may be in error when $\langle \delta C_p^{int} \rangle$ is not much smaller than $\langle \delta C_p^{trs} \rangle$ and, more generally, if the system deviates from the two-state behavior (Privalov and Potekhir, 1986).

Statistical thermodynamic treatment of the heat capacity function. At this point it is important to discuss the high informative potential of a statistical-mechanical treatment of DSC data. The strength of the DSC method is that it provides direct access to the system partition function without invoking *ad hoc* assumptions about the thermodynamic mechanism of conformational transition

[6] The vibrational content of the polypeptide chain increases upon unfolding, which also contributes to the positive value of ΔC_p^{den}. The magnitude of this effect is small in comparison to the hydration effect. Parametrisation of ΔC_p^{den} in terms of the change in solvent-accessible surface area has been based on thermodynamic data for the dissolution of model compounds. The parametrisation partly accounts for vibrational contributions.

[7] In the case of a simple two-state transition it is only the native and the denatured state.

[8] $\langle \delta C_p^{trs}(T) \rangle$ is a symmetric bell-shaped curve only for monomolecular transitions. In the case dissociation of a complex and unfolding of its components are coupled reactions, the heat capacity trace is skewed at the high-temperature shoulder. The maximum of the heat absorption peak, T_m, is higher than the temperature at which the transition is half-complete ($F_i = 0.5$, see the section 'Statistical thermodynamic treatment of the heat capacity function'.

(Freire and Biltonen, 1978a,b; Freire, 1994). For an arbitrary system containing N different states ($N = 2$ for a two-state transition), the system partition function is defined as:

$$Q = \sum_{i=1}^{N} K_i = \sum_{i=1}^{N} \exp\left(-\frac{\Delta G_i}{RT}\right) \tag{16}$$

The expression under the summation sign represents the statistical factors of each state. ΔG_i is defined by Eq. (1). The excess enthalpy of the system with respect to the native state is:

$$\langle \Delta H \rangle = \sum_{i=1}^{N} \Delta H_i F_i \tag{17}$$

where ΔH_i is the enthalpy of state i relative to the native reference state, and F_i is the population of state i in terms of the system partition function Q:

$$F_i = \frac{\exp\left(-\frac{\Delta G_i}{RT}\right)}{Q} \tag{18}$$

Since the excess heat capacity is the first derivative of the excess enthalpy with respect to the temperature, $\langle \Delta C_p \rangle$ can be expressed as:

$$\begin{aligned} \langle \Delta C_p \rangle &= \frac{\langle \Delta H \rangle}{\mathrm{d}T} = \frac{\sum_{i=1}^{N} (\Delta H_i F_i)}{\mathrm{d}T} \\ &= \sum_{i=1}^{N} \Delta C_{\mathrm{p}}^{\mathrm{den}} F_i + \sum_{i=1}^{N} \Delta H_i \frac{\mathrm{d}F_i}{\mathrm{d}T} \end{aligned} \tag{19a}$$

and after differentiation of $\mathrm{d}F_i/\mathrm{d}T$:

$$\begin{aligned} \langle \Delta C_p \rangle &= \frac{\langle \Delta H \rangle}{\mathrm{d}T} = \sum_{i=1}^{N} \Delta C_{\mathrm{p}}^{\mathrm{den}} F_i + \frac{\langle \Delta H^2 \rangle - \langle \Delta H \rangle^2}{RT^2} \\ &= \sum_{i=1}^{N} \langle \delta C_{\mathrm{p},i}^{\mathrm{int}} \rangle + \sum_{i=1}^{N} \langle \delta C_{\mathrm{p},i}^{\mathrm{trs}} \rangle \end{aligned} \tag{19b}$$

The statistical-mechanical treatment does not include arbitrary assumptions about the number of states populated in the transition process and about the mutual interaction of these states. The data can be rigorously tested against different thermodynamic models by variation of the definition of the partition function. Well-established statistical optimization procedures are used to find a model that best describes the experimental data. This approach has been successfully exploited to study complex unfolding processes (Montgomery *et al.*, 1993; Griko *et al.*, 1994a; Haynie and Freire, 1994; Johnson *et al.*, 1995).

Application of DSC to association reactions

How can we derive the energetic parameters of biological association reactions with the help of DSC data? If a ligand L binds to the native state of a protein M with high affinity, the heat capacity of the resulting complex LM will differ from that of M and L alone. As a consequence, the DSC profiles of L, M and ML will have distinct shapes. Dramatic deformations of the thermograms of proteins in the ligated state have been reported (Takahashi and Fukada, 1985; Shrake and Ross, 1990; Lin *et al.*, 1994; Conejero-Lara and Mateo, 1996). The influence of ligand binding on the stability of a whole protein, or a protein domain, can be large even if the ligand is a small organic compound. The situation is even more complicated when the ligand itself is a macromolecule undergoing conformational transition(s) with temperature. Furthermore, because the binding affinity and the stability of the complex partners and the complex itself are sensitive to pH, to ionic strength and to the nature of cosolutes, the excess heat capacity function, $\langle \Delta C_{\mathrm{p}}(T) \rangle$, can be distorted when the solvent conditions vary (Ramsay and Freire, 1990; Carra and Privalov, 1997). A careful deconvolution of the observed thermograms gives insight in the thermodynamic forces that drive the association reaction and can provide structural and mechanistic information about the interacting molecular species (Davis *et al.*, 1995; Litvinovich and Ingham, 1995; Filimonov and Rogov, 1996).

When the mutual stabilization of the complex partners in ML is high, the dissociation of the complex is tightly coupled to the denaturation of its components. The result is a single peak in the heat capacity trace at a temperature above the denaturation temperatures of L and M in isolation. Figure 4 shows an idealized example. In such a case, a simplified procedure can be applied to extract the enthalpy of complex formation. It involves extrapolation of the enthalpies of denaturation of the components to the melting temperature of the complex (Fukada *et al.*, 1985; Makarov

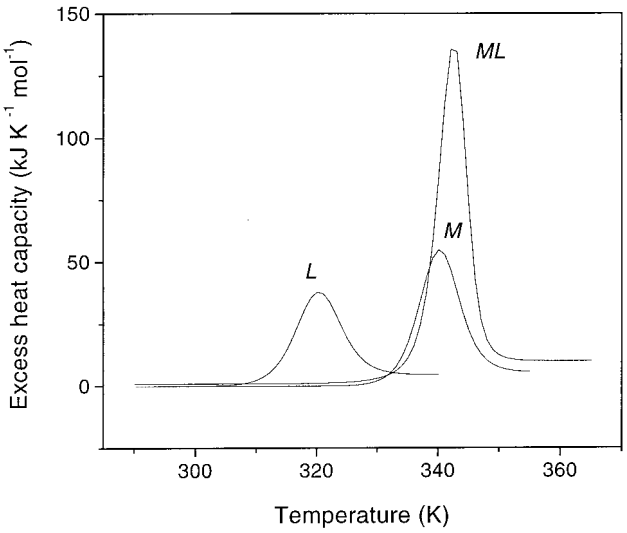

Figure 4. Simulated excess heat capacity profiles of ligand L, protein M and complex ML. In this idealized example, thermal transitions of L (T_m = 320 K) and M (T_m = 340 K) are well separated and lower than the thermal transition of the complex LM. Strong association leads to mutual stabilization of the complex partners in LM. The dissociation of the complex is tightly coupled to the denaturation of its components and a single peak appears in the heat capacity trace with T_m = 343 K, above the denaturation temperatures of L and M in isolation. The curves were calculated with the help of Eq. (22) for the conditions given in Fig. 5 with ΔH_c(298 K) = −20 kJ mol^{-1} and K_c(298 K) = 10^{10} M^{-1}.

et al., 1994; Yakovlev *et al.*, 1995). The energetics of complex formation can be studied also by investigating the dependence of ΔH_m and T_m on the saturation level of the system (Bhushan and McNamee, 1990; Shrake and Ross, 1990; Anteneodo *et al.*, 1994; Horvath *et al.*, 1994). However, in the majority of systems studied so far, the DSC trace has a complicated shape and exhibits several overlapping transitions. Moreover, even if the dissociation and the denaturation take place in a narrow temperature range, there is no a priori information about a possible redistribution of sub-states in the melting zone.

Deconvolution of DSC traces. The thermodynamic theory of deconvolution of coupled equilibria in macromolecular systems has been developed already with the first appearance of sensitive microcalorimeters. An extensive thermodynamic framework for extracting the free energy and enthalpy of binding from DSC data was first developed by Robert *et al.* (1989) and by Brandts and Lin (1990). More recently, the statistical-mechanical aspects of the deconvolution technique have been formulated by other investigators in the light of a global linkage analysis of two-dimensional heat capacity surfaces (by variation of temperature and ligand concentration; Ramsay and Freire, 1990; Straume and Freire, 1992; Straume, 1994; Barone *et al.*, 1995). The idea is to redefine the partition function of the system to account for the interaction between the molecules and then to use the standard expression of statistical thermodynamics, which is analogous to Eq. (5a), to calculate the excess enthalpy:

$$\frac{\delta \ln Q}{\delta T} = \frac{\langle \Delta H \rangle}{RT^2} \tag{20}$$

The relevant equations can be explicitly solved for only a few simple models, but numerical methods of non-linear optimization can help to adapt a particular model to the experimental data. To illustrate a strategy of how to deal with heat capacity traces, we again consider the simple case of interaction between L and M to the 1:1 complex ML, which we call C. The total concentrations are kept equal, $[L]_{tot} = [M]_{tot}$. The overall process is described by the following scheme:

$$\begin{array}{ccc} L_N & + & M_N \overset{K_C}{\rightleftarrows} C \\ K_L \uparrow\downarrow & & \uparrow\downarrow K_M \\ L_D & & M_D \end{array}$$

L and M exist in the native and the denatured form (subscripts $_N$ and $_D$, respectively). The free components are described by the following set of parameters (X denotes L or M): free energies of denaturation, ΔG_X; equilibrium denaturation constants, K_X; melting temperatures, T_{mX}; denaturation enthalpies, ΔH_{mX}; and heat capacity increments of denaturation, $\Delta C_{p,X}^{den}$. The parameters for the complex C are: free energy of binding, ΔG_C; binding constant, K_C; arbitrarily chosen reference temperature, $T_{R,C}$; enthalpy of complex formation, ΔH_C; and heat capacity change of binding, $\Delta C_{p,C}$. In what follows, two assumptions are made. Only L_N and M_N interact to form the complex C, and T_{mC} is always higher than T_{mX} as shown in the idealized example of Fig. 4. If this second condition is not fulfilled, the denaturation of L and/or M are/is not coupled to the binding equilibrium.

The partition function of the system describes the relative population of the native and denatured states of L, M and the population of C. Formally, we can write separate functions for L and M:

$$Q_L = 1 + K_L + K_C[M_N]$$

$$Q_M = 1 + K_M + K_C[L_N]$$

The two functions are coupled and the concentrations of L_N, M_N and C are:

$$[L_N] = \frac{[L]_{tot}}{Q_L}$$

$$[M_N] = \frac{[M]_{tot}}{Q_M}$$

$$[C] = K_C[L_N][M_N]$$

The concentrations of the free components, $[L_N]$ and $[M_N]$, can be solved simultaneously in terms of the known total concentrations and the equilibrium constants K_L, K_M and K_C, which are temperature dependent parameters according to (subscript $_X$ denotes L, M or C and subscript $_R$ a reference temperature):

$$K_X(T) = K_X(T_{R,X}) \exp\left[-\frac{\Delta H_{R,X}}{R}\left(\frac{1}{T} - \frac{1}{T_{R,X}}\right) + \frac{\Delta C_{p,X}}{R}\left(\ln\frac{T}{T_{R,X}} + \frac{T_{R,X}}{T} - 1\right)\right] \tag{21}$$

The excess enthalpy of the system, relative to the complex C as the reference state, for the given total concentrations $[L]_{tot}$ and $[M]_{tot}$, can be written in analogy to Eq. (17) as:

$$\langle \Delta H \rangle = \sum_{X=L,M}\left[\frac{K_X}{Q_X}\Delta H_X + \frac{K_X}{Q_X}\Delta C_{p,X}\right] - \frac{[C]}{[L]_{tot}}\Delta H_C - \frac{[C]}{[L]_{tot}}\Delta C_{p,C} \tag{22}$$

The last two terms in the above equation are correct only if $[L]_{tot} = [M]_{tot}$.[9] The combination of Eqs (21) and (22) describes the excess enthalpy function, $\langle \Delta H(T) \rangle$, of an associating system. From the combined equations, the excess heat capacity function, $\langle \Delta C_p(T) \rangle$, is calculated by either explicit or by numerical differentiation.

A set of simulations according to this general procedure is shown in Fig. 5. Panel A shows how the DSC trace is influenced by the stability of the complex (variation of K_C at fixed K_M and K_L). If the complex is weak, the thermogram shows the denaturation of free L and free M as two well separated thermal transitions. When the complex dominates, a single sharp peak at high temperature is seen because the dissociation of C and the denaturation of L and M are strongly coupled. For cases in between, the trace envelopes the dissociation of the complex and the denaturation of the free components. Panel B shows how the DSC trace changes

[9] If $[L]_{tot} \neq [M]_{tot}$, the binding polynomial has to be used to calculate the fraction of complex at each temperature.

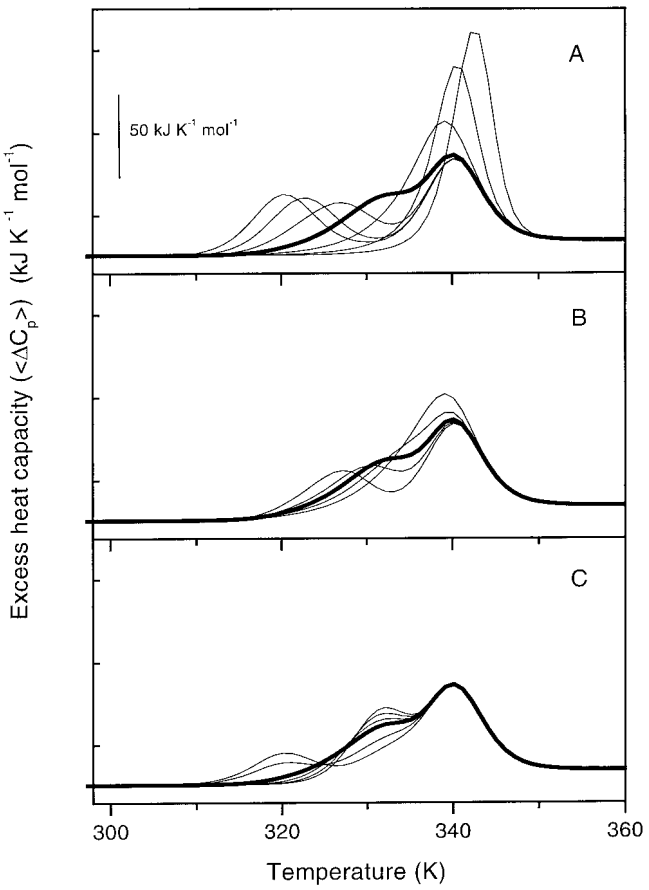

Figure 5. Simulated excess heat capacity profiles for the interacting system $L + M \rightarrow C$. The curves were simulated with the help of Eq. (22). The following parameters were fixed for all simulations: $T_{m,L} = 320$ K, $T_{m,M} = 340$ K, $\Delta H_L(T_m) = 350$ kJ mol^{-1}, $\Delta H_M(T_m) = 450$ kJ mol^{-1}, $\Delta C_{p,L} = 5.5$ kJ K^{-1} mol^{-1}, $\Delta C_{p,M} = 4.5$ kJ K^{-1} mol^{-1}, and $\Delta C_{p,C} = -1$ kJ K^{-1} mol^{-1}. The traces drawn in thick line are for identical conditions in all three panels. *Panel A*: variation of the DSC trace with variation of K_c. The curves from left to right were calculated for $K_c = 1$, 10^5, 10^6, 10^7, 10^8, 10^9, and 10^{10} M^{-1} at 298 K. The leftmost curve has two well-separated peaks centered at 320 and 340 K, respectively. The peaks correspond to the denaturation of free *L* and free *M*, respectively. The rightmost curve has a single peak centered at 343 K. It corresponds to the coupled dissociation and denaturation of the complex and its components, undisturbed by the presence of free *L* and *M*. The curves in between are composed to variable degrees of the transitions of the free and the complexed species. $\Delta H_{R,C}$ was fixed at -20 kJ mol^{-1} and 298 K. *Panel B*: variation of the DSC trace with variation of the excess enthalpy of the complex at the reference temperature 298 K. The curves from left to right were calculated for $\Delta H_{R,C} = 20$, 0, -20, -40, and -80 kJ mol^{-1} at 298 K. It is seen how the temperature influences K_C according to eqn (21). Hence, the overall trace of a DSC experiment changes with $\Delta H_{R,C}$. The leftmost trace calculated for $\Delta H_{R,C} = +20$ kJ mol^{-1} clearly has two peaks. The reason is that K_C decreases with increasing temperature if $\Delta H_{R,C}$ is positive, as follows from Eq. (21). Conversely, K_C increases with temperature if $\Delta H_{R,C} < 0$ and, therefore, the rightmost curve essentially has only a single peak, albeit with a broad shoulder. K_C was fixed at 10^7 M^{-1} at 298 K. *Panel C*: Variation of the DSC trace with variation of the ratio $[L]_{tot}/[M]_{tot}$. The curves from left to right were calculated for $[L]_{tot}/[M]_{tot} = 0.5$, 0.67, 1, 1.5, 2, and 4. ΔH_C(298 K) was fixed at -20 kJ mol^{-1} and K_C(298 K) at 10^7 M^{-1}.

with the magnitude of the enthalpy of complex formation, ΔH_C. From Eq. (21), it follows that K_C has a maximum at the temperature where $\Delta H_C = 0$, that is, where ΔH_C changes sign. Panel C demonstrates how the DSC trace changes with the molar ratio of $[L]_{tot}/[M]_{tot}$.

In practice, models can be tested against the experimental data by statistical methods. The statistical analysis is simpler if the unfolding enthalpies, unfolding heat capacity increments and unfolding free energies of each complex partner in isolation are known from separate DSC scans. Here, the statistical analysis of the DSC traces as shown in Fig. 5 can be limited to the parameters of the association reaction, keeping the parameters pertaining to the free components fixed. In principle, it is also possible to perform a global statistical analysis without a priori knowledge of some of the thermodynamic parameters. However, such rigorous statistical analysis by non-linear fitting procedures can be flawed because of the multi-minima problem when the number of parameters is large and some parameters are strongly interdependent.

Applications of the deconvolution analysis. Deconvolution analysis of DSC traces was successfully applied to study the energetics of small ligand binding like ferric ion binding to transferrins (Lin *et al.*, 1994), sulfate binding to yeast phosphoglycerate kinase (Hu and Sturtevant, 1989), and biotin binding to streptavidin (Gonzalez *et al.*, 1997). Other examples are inhibitor binding to barnase (Martinez *et al.*, 1994), to ribonuclease (Barone *et al.*, 1995), and to thymidylate synthase (Chen *et al.*, 1996), or monosaccharide binding to proteins (Schwarz *et al.*, 1993). In most cases good agreement was observed between the binding free energies determined by DSC and other equilibrium methods, and the superiority of DSC to measure binding affinities not accessible by other techniques was documented. Indeed, DSC allows to measure very tight binding, and this is a major asset of the technique compared to ITC and to non-calorimetric equilibrium techniques. The high resolution potential of the deconvolution of complex heat capacity traces was documented in studies of protein systems like the S-protein–S-peptide complex (Graziano *et al.*, 1996), the barnase–barstar complex (Martinez *et al.*, 1995), and the heparin/antithrombin complex (DeLauder *et al.*, 1992). Conformational transitions were found to accompany the dimerization of a thermolysin fragment (Conejero-Lara and Mateo, 1996), and the association of an unfolding intermediate of the Cro repressor from bacteriophage λ was identified (Filimonov and Rogov, 1996).

The statistical mechanical approach to DSC data was successfully applied to study the domain structure and domain-domain interactions in some very complicated molecular systems like the *Escherchia coli* DNA gyrase (Blandamer et al., 1994), the multimeric molecular chaperon DnaK (Montgomery *et al.*, 1993), and the heparin-binding fragment of fibronectin (Novokhatny *et al.*, 1992). Recent work on protein binding to single-stranded DNA and to DNA-duplexes illustrated the power of the combined ITC and DSC approach. Protein–DNA association is characterized by low discrimination between specific and nonspecific binding and by large structural rearrangements accompanying the binding reaction. The thermodynamic analysis of these complex systems could

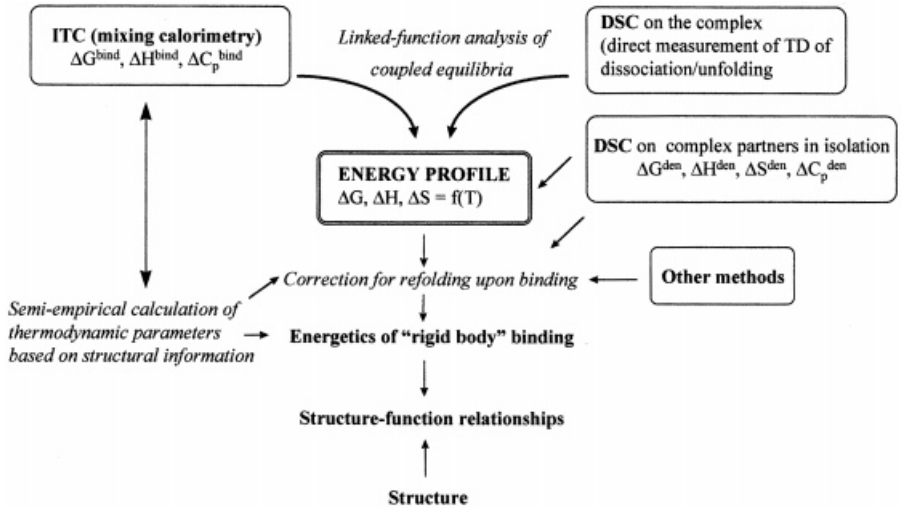

Figure 6. Scheme depicting the combined experimental and theoretical approach to the analysis of complex binding energetics. ITC provides the global thermodynamic parameters of the binding reaction (top left). Semi-empirical, structure-based calculations complement ITC data (lower left). DSC on the complex and on its free components (right hand side) can help to decompose the global parameters from ITC into contributions from conformational changes, folding of molecular domains, etc. Data from non-calorimetric methods complement the picture (bottom and lower right hand side). The energy profile of the binding reaction is the final result of the combined ITC-DSC approach (center) and a corner stone in the elucidation of structure–function relationships (bottom).

profit from the synergism of the ITC-DSC combination (Cooper *et al.*, 1994; Davis *et al.*, 1995; Merabet and Ackers, 1995; Carra and Privalov, 1997; Oda *et al.*, 1998).

Conclusions

We have tried to give an overview of the calorimetric techniques and to summarize some recent representative applications aimed at dissecting the energetics of macromolecular recognition. In view of the high sensitivity of commercially available instruments and of the capacity of molecular biology techniques and solid phase synthesis to produce large amounts of pure proteins and nucleic acids, the comprehensive thermodynamic description of a growing number of associating systems will become possible in the near future. Figure 6 illustrates how the power of ITC and DSC can be combined and linked with structural data. The central aim is to obtain an energy profile of the complex and to formulate a plausible mechanism of the association reaction. To know the energy profile means to know the heat capacity change of the association reaction and to predict the free energy, enthalpy, and entropy change of association over as broad a temperature range as possible and for varying conditions of solvent, pH, cosolutes, etc. To know the mechanism of the association reaction means to describe the transition from the free components to the final complex in terms of all intermediate states populated under equilibrium conditions, and to reveal their mutual interdependence.

ITC is clearly the method of choice to measure the free energy, enthalpy, heat capacity and stoichiometry of a binding reaction of modest affinity. Very weak and very tight binding constants are not directly accessible by ITC. Data collected by non-calorimetric methods are used to get van't Hoff enthalpies, which when compared with calorimetric enthalpies can help to clarify a binding mechanism. The quality of ΔH and ΔC_p from ITC is high when the association can be approximated by a rigid-body interaction. However, the lock-and-key concept is an oversimplification for many protein–protein complexes and is almost always inappropriate when applied to protein–DNA interactions. The resolution of ITC data can be improved substantially when the structure of the complex and of its free components is known (or a reasonable model can be proposed). In this case, semi-empirical, structure-based calculations can complement the experimental data. Still, these computational methods cannot (yet) replace experimental data. Here, the DSC technique comes to help. By deconvolution of the excess heat capacities of the interacting molecules one is in a position to ascribe at least part of the enthalpy and heat capacity measured by ITC to folding event(s) induced by the binding reaction. DSC data are invaluable in the estimation of entropic factors of a binding equilibrium and in measuring extremely high binding affinities. Statistical-mechanical analysis of two-dimensional excess heat capacity surfaces can provide further information on the nature of a complex and on the energetic factors driving its formation. DSC is the only method to access the system partition function to calculate the population of free and bound molecular species as a function of temperature and concentration.

Even the best and the most comprehensive set of thermodynamic data can be flawed, and we have tried to lay bare possible difficulties and inconsistencies of data analysis. Indeed, thermodynamic studies always need

company of additional studies based on other biochemical, structural and biophysical methods. As stated in the Introduction, we know much about *how* biomacromolecules associate and wish to better understand *why* they do so, but the *how* and *why* are strongly interdependent.

REFERENCES

Anteneodo, C., Rodahl, A. M, Meiering, E., Heynen, M. L, Sennisterra, G. A and Lepock, J. R (1994). Interaction of dibucaine with the transmembrane domain of the Ca(2+)-ATPase of sarcoplasmic reticulum. *Biochemistry* **33**, 12283–12290.

Ayala, Y. M, Vindigni, A., Nayal, M., Spolar, R. S, Record, Jr, M. T and Di Cera, E. (1995). Thermodynamic investigation of hirudin binding to the slow and fast forms of thrombin: evidence for folding transitions in the inhibitor and protease coupled to binding. *J. Molec. Biol.* **253**, 787–798.

Baker, B. M and Murphy, K. P (1996). Evaluation of linked protonation effects in protein binding reactions using isothermal titration calorimetry. *Biophys. J.* **71**, 2049–2055.

Baker, B. M and Murphy, K. P (1997). Dissecting the energetics of a protein-protein interaction: the binding of ovomucoid third domain to elastase. *J. Molec. Biol.* **268**, 557–569.

Barone, G., Catanzano, F., Del Vecchio, P., Giancola, C. and Graziano, G. (1995). Differential scanning calorimetry as a tool to study protein-ligand interactions. *Pure Appl. Chem.* **67**, 1867.

Berger, C., Jelesarov, I. and Bosshard, H. R (1996). Coupled folding and site-specific binding of the GCN4-bZIP transcription factor to the AP-1 and ATF/CREB DNA sites studied by microcalorimetry. *Biochemistry* **35**, 14984–14991.

Berglund, H., Wolf-Watz, M., Lundback, T., van den Berg, S. and Hard, T. (1997). Structure and dynamics of the glucocorticoid receptor DNA-binding domain: comparison of wild type and a mutant with altered specificity. *Biochemistry* **36**, 11188–11197.

Bhat, T. N, Bentley, G. A, Boulot, G., Greene, M. I, Tello, D., Dall'Acqua, W., Souchon, H., Schwarz, F. P, Mariuzza, R. A and Poljak, R. J (1994). Bound water molecules and conformational stabilization help mediate an antigen-antibody association. *Proc. Natl Acad. Sci. USA* **91**, 1089–1093.

Bhushan, A. and McNamee, M. G (1990). Differential scanning calorimetry and Fourier transform infrared analysis of lipid–protein interactions involving the nicotinic acetylcholine receptor. *Biochim. Biophys. Acta* **1027**, 93–101.

Blandamer, M. J, Briggs, B., Cullis, P. M, Jackson, A. P, Maxwell, A. and Reece, R. J (1994). Domain structure of Escherichia coli DNA gyrase as revealed by differential scanning calorimetry. *Biochemistry* **33**, 7510–7516.

Boresch, S. and Karplus, M. (1995). The meaning of component analysis: decomposition of the free energy in terms of specific interactions. *J. Molec. Biol.* **254**, 801–807.

Botuyan, M. V, Keire, D. A, Kroen, C. and Gorenstein, D. G (1993). ^{31}P nuclear magnetic resonance spectra and dissociation constants of lac repressor headpiece duplex operator complexes: the importance of phosphate backbone flexibility in protein–DNA recognition. *Biochemistry* **32**, 6863–6874.

Brady, G. P and Sharp, K. A (1995). Decomposition of interaction free energies in proteins and other complex systems. *J. Molec. Biol.* **254**, 77–85.

Brandts, J. F and Lin, L. N (1990). Study of strong to ultratight protein interactions using differential scanning calorimetry. *Biochemistry* **29**, 6927–6940.

Breslauer, K. J, Freire, E. and Straume, M. (1992). Calorimetry: a tool for DNA and ligand–DNA studies. *Methods Enzymol.* **211**, 533–567.

Bruzzese, F. J and Connelly, P. R (1997). Allosteric properties of inosine monophosphate dehydrogenase revealed through the thermodynamics of binding of inosine 5′-monophosphate and mycophenolic acid. Temperature dependent heat capacity of binding as a signature of ligand-coupled conformational equilibria. *Biochemistry* **36**, 10428–10438.

Bundle, D. R and Sigurskjold, B. W (1994). Determination of accurate thermodynamics of binding by titration microcalorimetry. *Meth. Enzymol.* **247**, 288–305.

Carra, J. H and Privalov, P. L (1997). Energetics of folding and DNA binding of the MAT α2 homeodomain. *Biochemistry* **36**, 526–535.

Chaires, J. B (1997). Possible origin of differences between van't Hoff and calorimetric enthalpy estimates. *Biophys. Chem.* **64**, 15–23.

Chen, C. H, Davis, R. A and Maley, F. (1996). Thermodynamic stabilization of nucleotide binding to thymidylate synthase by a potent benzoquinazoline folate analogue inhibitor. *Biochemistry* **35**, 8786–8793.

Chervenak, M. C and Toone, E. J (1994). A direct measure of the contribution of solvent reorganization to the enthalpy of ligand binding. *J. Am. Chem. Soc.* **116**, 10533–10539.

Christensen, J. J, Hansen, L. D and Izatt, R. M (1976). Handbook of Proton Ionization Heats and Related Thermodynamic Quantities, Wiley, New York.

Collins, K. D (1997). Charge density-dependent strength of hydration and biological structure. *Biophys. J.* **72**, 65–76.

Conejero-Lara, F. and Mateo, P. L (1996). Presence of a slow dimerization equilibrium on the thermal unfolding of the 205–316 thermolysin fragment at neutral pH. *Biochemistry* **35**, 3477–3486.

Connelly, P. R (1994). Acquisition and use of calorimetric data for prediction of the thermodynamics of ligand-binding and folding reactions of proteins. *Curr. Opin. Biotechnol.* **5**, 381–388.

Connelly, P. R, Aldape, R. A, Bruzzese, F. J, Chambers, S. P, Fitzgibbon, M. J, Fleming, M. A, Itoh, S., Livingston, D. J, Navia, M. A, Thomson, J. A and Wilson, K. P (1994). Enthalpy of hydrogen bond formation in a protein-ligand binding reaction. *Proc. Natl Acad. Sci. USA* **91**, 1964–1968.

Connelly, P. R, Thomson, J. A, Fitzgibbon, M. J and Bruzzese, F. J (1993). Probing hydration contributions to the thermodynamics of ligand binding by proteins. Enthalpy and heat capacity changes of tacrolimus and rapamycin binding to FK506 binding protein in D_2O and H_2O. *Biochemistry* **32**, 5583–5590.

Connelly, P. R and Thomson, J. A (1992). Heat capacity changes and hydrophobic interactions in the binding of FK506 and rapamycin to the FK506 binding protein. *Proc. Natl Acad. Sci. USA* **89**, 4781–4785.

Cooper, A., McAlpine, A. and Stockley, P. G (1994). Calorimetric studies of the energetics of protein–DNA interactions in the E. coli methionine repressor (MetJ) system. *FEBS Lett.* **348**, 41–45.

Davis, K. G, Plyte, S. E, Robertson, S. R, Cooper, A. and Kneale, G. G (1995). Comparison of Pf1 and Fd gene 5 proteins and their single-stranded DNA complexes by NMR spectroscopy and differential scanning calorimetry. *Biochemistry* **34**, 148–154.

DeLauder, S., Schwarz, F. P, Williams, J. CSr. and Atha, D. H (1992). Thermodynamic analysis of heparin binding to human antithrombin. *Biochim. Biophys. Acta* **1159**, 141–149.

Doyle, M. L, Louie, G., Dal Monte, P. R and Sokoloski, T. D (1995). Tight binding affinities determined from thermodynamic linkage to protons by titration calorimetry. *Methods Enzymol.* **259**, 183–194.

Dunitz, J. D (1995). Win some, lose some. Enthalpy-entropy compensation in weak intermolecular interactions. *Chem. Biol.* **2**, 709–712.

Eisenstein, E., Yu, H. D and Schwarz, F. P (1994). Cooperative binding of the feedback modifiers isoleucine and valine to biosynthetic threonine deaminase from Escherichia coli. *J.*

Biol. Chem. **269**, 29423–29429.
Faergeman, N. J, Sigurskjold, B. W, Kragelund, B. B, Andersen, K. V and Knudsen, J. (1996). Thermodynamics of ligand binding to acyl-coenzyme. A binding protein studied by titration calorimetry. *Biochemistry* **35**, 14118–14126.
Ferrari, M. E and Lohman, T. M (1994). Apparent heat capacity change accompanying a nonspecific protein-DNA interaction. Escherichia coli SSB tetramer binding to oligodeoxyadenylates. *Biochemistry* **33**, 12896–12910.
Filimonov, V. V and Rogov, V. V (1996). Reversible association of the equilibrium unfolding intermediate of lambda Cro repressor. *J. Molec. Biol.* **255**, 767–777.
Freire, E. (1994). Statistical thermodynamic analysis of differential scanning calorimetry data: structural deconvolution of heat capacity function of proteins. *Methods Enzymol.* **240**, 502–530.
Freire, E. (1995). Differential scanning calorimetry. *Meth. Molec. Biol.* **40**, 191–218.
Freire, E. and Biltonen, R. L (1978a). Statistical mechanical deconvolution of thermal transitions in macromolecules. I. Theory and application to homogeneous systems. *Biopolymers* **17**, 463–479.
Freire, E. and Biltonen, R. L (1978b). Statistical mechanical deconvolution of thermal transitions in macromolecules. II. General treatment of cooperative phenomena. *Biopolymers* **17**, 481–496.
Freire, E., Mayorga, O. L and Straume, M. (1990). Isothermal titration calorimetry. *Anal. Chem.* **62**, 950A–959A.
Frisch, C., Schreiber, G., Johnson, C. M and Fersht, A. R (1997). Thermodynamics of the interaction of barnase and barstar: changes in free energy versus changes in enthalpy on mutation. *J. Molec. Biol.* **267**, 696–706.
Fukada, H., Takahashi, K. and Sturtevant, J. M (1985). Thermodynamics of the binding of Streptomyces subtilisin inhibitor to α-chymotrypsin. *Biochemistry* **24**, 5109–5115.
Gilli, P., Ferretti, V. and Gilli, G. (1994). Enthalpy-entropy compensation in drug-receptor binding. *J. Phys. Chem.* **98**, 1515–1518.
Goldbaum, F. A, Schwarz, F. P, Eisenstein, E., Cauerhff, A., Mariuzza, R. A and Poljak, R. J (1996). The effect of water activity on the association constant and the enthalpy of reaction between lysozyme and the specific antibodies D1.3 and D44.1. *J. Mol. Recognit.* **9**, 6–12.
Gomez, J. and Freire, E. (1995). Thermodynamic mapping of the inhibitor site of the aspartic protease endothiapepsin. *J. Mol. Biol.* **252**, 337–350.
Gomez, J., Hilser, V. J, Xie, D. and Freire, E. (1995). The heat capacity of proteins. *Proteins* **22**, 404–412.
Gonzalez, M., Bagatolli, L. A, Echabe, I., Arrondo, J. L. R., Argarana, C. E, Cantor, C. R and Fidelio, G. D (1997). Interaction of biotin with streptavidin. Thermostability and conformational changes upon binding. *J. Biol. Chem.* **272**, 11288–11294.
Gopal, B., Swaminathan, C. P, Bhattacharya, S., Bhattacharya, A., Murthy, M. R and Surolia, A. (1997). Thermodynamics of metal ion binding and denaturation of a calcium binding protein from Entamoeba histolytica. *Biochemistry* **36**, 10910–10916.
Graziano, G., Catanzano, F., Giancola, C. and Barone, G. (1996). DSC study of the thermal stability of S-protein and S-peptide/S-protein. *Biochemistry* **35**, 13386–13392.
Griko, Y. V, Freire, E. and Privalov, P. L (1994a). Energetics of the -lactalbumin states: a calorimetric and statistical thermodynamic study. *Biochemistry* **33**, 1889–1899.
Griko, Y. V, Makhatadze, G. I, Privalov, P. L and Hartley, R. W (1994b). Thermodynamics of barnase unfolding. *Protein Sci.* **3**, 669–676.
Haynie, D. T and Freire, E. (1994). Estimation of the folding/unfolding energetics of marginally stable proteins using differential scanning calorimetry. *Anal. Biochem.* **216**, 33–41.
Holdgate, G. A, Tunnicliffe, A., Ward, W. H, Weston, S. A, Rosenbrock, G., Barth, P. T, Taylor, I. W, Pauptit, R. A and Timms, D. (1997). The entropic penalty of ordered water accounts for weaker binding of the antibiotic novobiocin to a resistant mutant of DNA gyrase: a thermodynamic and crystallographic study. *Biochemistry* **36**, 9663–9673.
Horvath, L. A, Sturtevant, J. M and Prestegard, J. H (1994). Kinetics and thermodynamics of thermal denaturation in acyl carrier protein. *Protein Sci.* **3**, 103–108.
Hu, C. Q and Sturtevant, J. M (1989). A differential scanning calorimetric study of the binding of sulfate ion and of Cibacron blue F3GA to yeast phosphoglycerate kinase. *Biochemistry* **28**, 813–818.
Hu, D. D and Eftink, M. R (1994). Thermodynamic studies of the interaction of trp aporepressor with tryptophan analogs. *Biophys. Chem.* **49**, 233–239.
Hyre, D. E and Spicer, L. D (1995). Thermodynamic evaluation of binding interactions in the methionine repressor system of Escherichia coli using isothermal titration calorimetry. *Biochemistry* **34**, 3212–3221.
Ito, W., Iba, Y. and Kurosawa, Y. (1993). Effects of substitutions of closely related amino acids at the contact surface in an antigen–antibody complex on thermodynamic parameters. *J. Biol. Chem.* **268**, 16639–16647.
Jelesarov, I. and Bosshard, H. R (1994). Thermodynamics of ferredoxin binding to ferredoxin:$NADP^+$ reductase and the role of water at the complex interface. *Biochemistry* **33**, 13321–13328.
Jelesarov, I., Dürr, E. and Bosshard, H. R (1998). Salt effects on hydrophobic interaction and charge screening in the folding of a negatively charged peptide to a coiled coil (leucine zipper). *Biochemistry* **37**, 7539–7550.
Jin, L., Yang, J. and Carey, J. (1993). Thermodynamics of ligand binding to trp repressor. *Biochemistry* **32**, 7302–7309.
Johnson, C. R, Morin, P. E, Arrowsmith, C. H and Freire, E. (1995). Thermodynamic analysis of the structural stability of the tetrameric oligomerization domain of p53 tumor suppressor. *Biochemistry* **34**, 5309–5316.
Kauzmann, W. (1959). Some factors in the interpretation of protein denaturation. *Adv. Protein Chem.* **14**, 1–63.
Kavanoor, M. and Eftink, M. R (1997). Characterization of the role of side-chain interactions in the binding of ligands to apo trp repressor: pH dependence studies. *Biophys. Chem.* **66**, 43–55.
Khalifah, R. G, Zhang, F., Parr, J. S and Rowe, E. S (1993). Thermodynamics of binding of the CO_2-competitive inhibitor imidazole and related compounds to human carbonic anhydrase I: an isothermal titration calorimetry approach to studying weak binding by displacement with strong inhibitors. *Biochemistry* **32**, 3058–3066.
Kornblatt, J. A, Kornblatt, M. J, Hoa, G.HB and Mauk, A. G (1993). Responses of two protein–protein complexes to solvent stress: does water play a role at the interface. *Biophys. J.* **65**, 1059–1065.
Kresheck, G. C, Vitello, L. B and Erman, J. E (1995). Calorimetric studies on the interaction of horse ferricytochrome c and yeast cytochrome c peroxidase. *Biochemistry* **34**, 8398–8405.
Ladbury, J. E (1996). Just add water: The effect of water on the specificity of protein-ligand binding sites and its potential application to drug design. *Chem. Biol.* **3**, 973–980.
Ladbury, J. E, Wright, J. G, Sturtevant, J. M and Sigler, P. B (1994). A thermodynamic study of the trp repressor-operator interaction. *J. Mol. Biol.* **238**, 669–681.
Lin, L. N, Mason, A. B, Woodworth, R. C and Brandts, J. F (1994). Calorimetric studies of serum transferrin and ovotransferrin. Estimates of domain interactions, and study of the kinetic complexities of ferric ion binding. *Biochemistry* **33**, 1881–1888.
Litvinovich, S. V and Ingham, K. C (1995). Interactions between type III domains in the 110 kDa cell-binding fragment of fibronectin. *J. Mol. Biol.* **248**, 611–626.
Lumry, R. and Rajender, S. (1970). Enthalpy-entropy compensation phenomena in water solutions of proteins and small molecules: a ubiquitous property of water. *Biopolymers* **9**, 1125–1227.
Lundbäck, T., Hansson, H., Knapp, S., Ladenstein, R. and Hard, T. (1998). Thermodynamic characterization of non-sequence-specific DNA-binding by the Sso7d protein from Sulfolobus solfactorius. *J. Mol. Biol.* **276**, 775–786.
Makarov, A. A, Protasevich, I. I, Lobachov, V. M, Kirpichnikov, M.

P, Yakovlev, G. I, Gilli, R. M, Briand, C. M and Hartley, R. W (1994). Thermostability of the barnase–barstar complex. *FEBS Lett.* **354**, 251–254.
Makhatadze, G. I and Privalov, P. L (1995). Energetics of protein structure. *Adv. Protein Chem.* **47**, 307–425.
Mark, A. E and van Gunsteren, W. F (1994). Decomposition of the free energy of a system in terms of specific interactions. *J. Mol. Biol.* **240**, 167–176.
Martinez, J. C, el Harrous, M., Filimonov, V. V, Mateo, P. L and Fersht, A. R (1994). A calorimetric study of the thermal stability of barnase and its interaction with 3′GMP. *Biochemistry* **33**, 3919–3926.
Martinez, J. C, Filimonov, V. V, Mateo, P. L, Schreiber, G. and Fersht, A. R (1995). A calorimetric study of the thermal stability of barstar and its interaction with barnase. *Biochemistry* **34**, 5224–5233.
McKinnon, I. R, Fall, L., Parody-Morreale, A. and Gill, S. J (1984). A twin titration microcalorimeter for the study of biochemical reactions. *Anal. Biochem.* **139**, 134–139.
McNemar, C., Snow, M. E, Windsor, W. T, Prongay, A., Mui, P., Zhang, R., Durkin, J., Le, H. V and Weber, P. C (1997). Thermodynamic and structural analysis of phosphotyrosine polypeptide binding to Grb2-SH2. *Biochemistry* **36**, 10006–10014.
Merabet, E. and Ackers, G. K (1995). Calorimetric analysis of lambda cI repressor binding to DNA operator sites. *Biochemistry* **34**, 8554–8563.
Montgomery, D., Jordan, R., McMacken, R. and Freire, E. (1993). Thermodynamic and structural analysis of the folding/unfolding transitions of the Escherichia coli molecular chaperone DnaK. *J. Mol. Biol.* **232**, 680–692.
Murphy, K. P and Freire, E. (1992). Thermodynamics of structural stability and cooperative folding behavior in proteins. *Adv. Protein Chem.* **43**, 313–361.
Murphy, K. P, Xie, D., Garcia, K. C, Amzel, L. M and Freire, E. (1993). Structural energetics of peptide recognition: angiotensin II/antibody binding. *Proteins* **15**, 113–120.
Murphy, K. P, Xie, D., Thompson, K. S, Amzel, L. M and Freire, E. (1994). Entropy in biological binding processes: estimation of translational entropy loss. *Proteins* **18**, 63–67.
Naghibi, H., Tamura, A. and Sturtevant, J. M (1995). Significant discrepancies between van't Hoff and calorimetric enthalpies. *Proc. Natl. Acad. Sci. USA* **92**, 5597–5599.
Novokhatny, V., Schwarz, F., Atha, D. and Ingham, K. (1992). Domain structure and domain-domain interactions in the carboxy-terminal heparin binding region of fibronectin. *J. Mol. Biol.* **227**, 1182–1191.
Oda, M., Furukawa, K., Ogata, K., Sarai, A. and Nakamura, H. (1998). Thermodynamics of specific and non-specific DNA binding by the c-Myb DNA-binding domain. *J. Mol. Biol.* **276**, 571–590.
Padlan, E. A (1996). X-ray crystallography of antibodies. *Adv. Protein Chem.* **49**, 57–133.
Patikoglou, G. and Burley, S. K (1997). Eukaryotic transcription factor–DNA complexes. *Annu. Rev. Biophys. Biomol. Struct.* **26**, 289–325.
Pearce, K. HJr, Ultsch, M. H, Kelley, R. F, de Vos, A. M and Wells, J. A (1996). Structural and mutational analysis of affinity-inert contact residues at the growth hormone-receptor interface. *Biochemistry* **35**, 10300–10307.
Plum, G. E and Breslauer, K. J (1995). Calorimetry of proteins and nucleic acids. *Curr. Opin. Struct. Biol.* **5**, 682–690.
Privalov, P. L and Makhatadze, G. I (1990). Heat capacity of proteins. II. Partial molar heat capacity of the unfolded polypeptide chain of proteins: protein unfolding effects. *J. Mol. Biol.* **213**, 385–391.
Privalov, P. L and Potekhin, S. A (1986). Scanning microcalorimetry in studying temperature-induced changes in proteins. *Methods Enzymol.* **131**, 4–51.
Ramsay, G. and Freire, E. (1990). Linked thermal and solute perturbation analysis of cooperative domain interactions in proteins. Structural stability of diphtheria toxin. *Biochemistry* **29**, 8677–8683.
Robert, C. H, Colosimo, A. and Gill, S. J (1989). Allosteric formulation of thermal transitions in macromolecules, including effects of ligand binding and oligomerization. *Biopolymers* **28**, 1705–1729.
Robinson, C. R and Sligar, S. G (1993). Molecular recognition mediated by bound water. A mechanism for star activity of the restriction endonuclease EcoRI. *J. Mol. Biol.* **234**, 302–306.
Schwarz, F. P, Puri, K. D, Bhat, R. G and Surolia, A. (1993). Thermodynamics of monosaccharide binding to concanavalin A, pea (Pisum sativum) lectin, and lentil (Lens culinaris) lectin. *J. Biol. Chem.* **268**, 7668–7677.
Shrake, A. and Ross, P. D (1990). Ligand-induced biphasic protein denaturation. *J. Biol. Chem.* **265**, 5055–5059.
Sigurskjold, B. W, Berland, C. R and Svensson, B. (1994). Thermodynamics of inhibitor binding to the catalytic site of glucoamylase from Aspergillus niger determined by displacement titration calorimetry. *Biochemistry* **33**, 10191–10199.
Spolar, R. S and Record, M. TJr. (1994). Coupling of local folding to site-specific binding of proteins to DNA. *Science* **263**, 777–784.
Spolar, R. S, Livingstone, J. R and Record M. TJr., (1992). Use of liquid hydrocarbon and amide transfer data to estimate contributions to thermodynamic functions of protein folding from the removal of nonpolar and polar surface from water. *Biochemistry* **31**, 3947–3955.
Straume, M. (1994). Analysis of two-dimensional differential scanning calorimetry data: elucidation of complex biomolecular energetics. *Methods Enzymol.* **240**, 530–568.
Straume, M. and Freire, E. (1992). Two-dimensional differential scanning calorimetry: simultaneous resolution of intrinsic protein structural energetics and ligand binding interactions by global linkage analysis. *Anal. Biochem.* **203**, 259–268.
Sturtevant, J. M (1977). Heat capacity and entropy changes in processes involving proteins. *Proc. Natl. Acad. Sci. USA* **74**, 2236–2240.
Sturtevant, J. M (1987). Biochemical applications of differential scanning calorimetry. *Ann. Rev. Phys. Chem.* **38**, 463–488.
Takahashi, K. and Fukada, H. (1985). Calorimetric studies of the binding of Streptomyces subtilisin inhibitor to subtilisin of Bacillus subtilis strain N′. *Biochemistry* **24**, 297–300.
Tamura, A. and Privalov, P. L (1997). The entropy cost of protein association. *J. Mol. Biol.* **273**, 1048–1060.
Tidor, B. and Karplus, M. (1994). The contribution of vibrational entropy to molecular association. The dimerization of insulin. *J. Mol. Biol.* **238**, 405–414.
van Oss, C. J (1997). Kinetics and energetics of specific intermolecular interactions. *J. Mol. Recognit.* **10**, 203–218.
Viguera, A. R, Martinez, J. C, Filimonov, V. V, Mateo, P. L and Serrano, L. (1994). Thermodynamic and kinetic analysis of the SH3 domain of spectrin shows a two-state folding transition. *Biochemistry* **33**, 2142–2150.
Wintrode, P. L and Privalov, P. L (1997). Energetics of target peptide recognition by calmodulin: a calorimetric study. *J. Mol. Biol.* **266**, 1050–1062.
Wiseman, T., Williston, S., Brandts, J. F and Lin, L. N (1989). Rapid measurement of binding constants and heats of binding using a new titration calorimeter. *Anal. Biochem.* **179**, 131–137.
Wyman, J. and Gill, S. J (1990). Binding and Linkage: Functional Chemistry of Biological Macromolecules. University Science Books, Mill Valley, CA.
Xavier, K. A, Shick, K. A, Smith-Gill, S. J and Willson, R. C (1997). Involvement of water molecules in the association of monoclonal antibody HyHEL-5 with bobwhite quail lysozyme. *Biophys. J.* **73**, 2116–2125.
Xie, D., Fox, R. and Freire, E. (1994). Thermodynamic characterization of an equilibrium folding intermediate of staphylococcal nuclease. *Protein Sci.* **3**, 2175–2184.
Yakovlev, G. I, Moiseyev, G. P, Protasevich, I. I, Ranjbar, B., Bocharov, A. L, Kirpichnikov, M. P, Gilli, R. M, Briand, C. M, Hartley, R. W and Makarov, A. A (1995). Dissociation constants and thermal stability of complexes of Bacillus intermedius RNase and the protein inhibitor of Bacillus amyloliquefaciens RNase. *FEBS Lett.* **366**, 156–158.

